IEEE Access
Multidisciplinary | Rapid Review | Open Access Journal

Received April 4, 2019, accepted June 29, 2019, date of publication July 10, 2019, date of current version July 26, 2019.

Digital Object Identifier 10.1109/ACCESS.2019.2927445

Detection Test for Periodic Signals Revisited Against Various Stochastic Models

CHANG XU
School of Geomatics and Municipal Engineering, Zhejiang University of Water Resources and Electric Power, Hangzhou 310018, China
e-mail: xuchang404@163.com

This work was supported by the National Natural Science Foundation of China, under Grant 41804007.

ABSTRACT Appropriate noise background should be taken into account when searching for the periodic or quasi-periodic oscillation buried in red noise. Null hypothesis assuming a conventional first-order autoregressive (AR(1)) process may lead to misleading conclusions since we know from many other studies that the noise in astrophysical and geographical sources exhibit the Fourier power-law-like properties. We improve the detection of periodic signals with the multitaper spectrum and wavelet spectrum by systematically taking into account a more appropriate null hypothesis (noise background) along with the multiple testing to test against. The confident level is determined with the noise contents obtained by using the maximum likelihood estimation (MLE) technique in the time domain, along with the data error covariance constructed using the fractional differencing. Not only traditional AR(1), but also the generalized Gauss–Markov, power law, and autoregressive fractionally integrated moving average (ARFIMA) process are included as possible candidate null hypothesis. The Bayesian Information Criterion (BIC) is adopted to quantify how well the candidate noise models fit the data under consideration. Our method is demonstrated on pre-seismic electromagnetic emissions, weight-percentage calcium carbonate data, and sea surface temperature anomaly variability. The result shows that our approach has a more extensive value of the application.

INDEX TERMS Hypothesis test, noise, MLE, wavelet, multitaper method.

I. INTRODUCTION

Detection and significance estimation of periodic or quasi-periodic oscillation (QPO) from intrinsic variability in the climatic, geophysical and astrophysical source have received much attention for over several decades. However, random errors of observation (typically white, and often complicated by the presence of systematic errors) and intrinsic random source variability (e.g. with a characteristic 'red' noise background) dominated in the observations greatly complicate the process of searching for possible weak oscillatory components. In principle, harmonic or narrowband spectral features isolated in the spectrum relative to a suitably defined null hypothesis (noise background) are considered to be statistical significant with a certain percent confidence. The confidence levels (CLs) are linked to a priori assumption regarding the nature of the noise background, and the significance thresholds are usually determined from the appropriate quantiles of the chi-squared distribution or Monte Carlo (MC) tests. Due to the ease of implementation, a first-order autoregressive (henceforth AR(1)) process is often assumed to accommodate the red noise background assumption requisite in many science scenarios, particularly climatic. To the best of our knowledge, the publicly available wavelet-based computer program developed by Torrence and Compo [1] (hereafter TC98) and the legacy singular spectral analysis-multitaper method (SSA-MTM) toolkit [2] (where the MTM-based algorithm [3] and MCSSA [4] are implemented) are widely used in a variety of scientific fields, with over 1000 citations in the Web of Science. However, the default noise model (i.e., AR(1)) built in currently TC98 and SSA-MTM Toolkit may be insufficient to characterize the noise background of some astrophysical sources and geodetic records, where power law (PL) or bending PL is extremely common in nature (see e.g., [5], [6] and references therein). Consequently, neglecting the noise background nature of the observed spectrum and directly using TC98 and SSA-MTM as a pure black box may lead to false detections and incorrect conclusions. The elementary step of estimating and checking the null hypothesis (i.e. background noise) is strongly recommended

The associate editor coordinating the review of this manuscript and approving it for publication was Lei Wu.

and highlighted in [7] and [8]. Such issue is usually ignored in the standard significance tests, and it seems worthwhile to re-examine the periodic phenomena in several previously published reports. In our previous paper [9], we adapt the TC98 method to take into account the generalized Gauss Markov (GGM) stochastic model [10] which includes a AR(1) and PL process as special cases. In this study, we plane to further discuss the periodic signals detection using multitaper and wavelet spectrum analysis but extend them with a more general non-Gaussian correlated noise as null hypothesis to test against, where the CLs are determined with the noise contents obtained by using the maximum likelihood estimation (MLE) technique in the time domain, along with the data error covariance constructed with the fractional differencing [11]. Inspired by the original methods employed in [10], [12] and [13], not only will GGM noise model, but other noise models including PL, AR(1) and autoregressive fractionally integrated moving average (ARFIMA) [14] will be reexamined as possible candidate null hypothesis to determine the appropriate CLs for the existence of periodic or quasi-periodic signals. Furthermore, we pick up from where we left off in our earlier paper [9] and discuss the multiple testing effects in the wavelet spectrum, since we know that the pointwize significance tests adopted in TC98 may generate false positives results (for details, see [15]).

The rest of the article is structured as follows. Section 2 describes the stochastic models and their covariance matrices with applications to real data. Section 3 discusses the real data (e.g., electromagnetic emission (EME) time series, stratigraphic data and sea surface temperature (SST) anomaly) and quantifies the performance of our algorithms to examine the evidence for cycles in each. Finally, Section 4 concludes and outlines ideas for further work.

II. CANDIDATE STOCHASTIC MODELS

Spectrum fitting in the frequency domain is a straightforward method to estimate the noise in data (see e.g., [16], [17] and [5]). Here we focus on the MLE technique in the time domain to estimate the stochastic noise components, because MLE has two advantages over spectrum fitting: (1) can work with gappy data, (2) no windowing and spectral averaging required [10]. Furthermore, using a fast Toeplitz solver and recursive procedures proposed by Bos *et al.* [18], the stochastic noise components can be estimated by MLE without any computational burden.

We make the usual assumption that the data can be well modeled by a sum of deterministic (including trend and periodic oscillation) and stochastic terms

$$y(t_i)=a+bt_i+\sum_{k=1}^{K}[c_k\sin(2\pi f_k t_i)+d_k\cos(2\pi f_k t_i)]+\varepsilon_i \quad (1)$$

where a is the intercept; b is linear rate; t_i is time epoch; the coefficients c_k and d_k are sine and cosine amplitudes at frequency f_k; and ε is a vector of independent measurement errors.

Then the noise components can be estimated by maximizing the probability function by adjusting the data covariance

$$\mathrm{lik}(\hat{v},\mathrm{C})=\frac{1}{(2\pi)^{N/2}(\det(\mathrm{C}))^{1/2}}\exp(-0.5\hat{v}^{\mathrm{T}}\mathrm{C}^{-1}\hat{v}) \quad (2)$$

or

$$\ln[\mathrm{lik}(\hat{v},\mathrm{C})]=-\frac{1}{2}\left[N\ln(2\pi)+\ln(\det(\mathrm{C})+\hat{v}\mathrm{C}^{-1}\hat{v})\right] \quad (3)$$

where det is the determinant of a matrix, C is the covariance matrix representing the assumed noise in the data, N is the number of epochs (gaps do not count) and $\hat{v}$ are the postfit residuals to the linear function using weighted least squares with the same covariance matrix C. As can be seen from the above, our MLE method has the advantage of avoiding the potential biased noise estimation problem caused by a strong trend and (quasi) periodic signals, a circumstance that is presumed common in geophysical, astrophysical, and cyclostratigraphic records.

Following [12], we construct the covariance matrix using the variance in front of the sum of the many matrices and introducing the fraction parameter $\phi \in [0, 1]$ to control the distribution of each noise model:

$$\mathrm{C}=\sigma^2(\phi_1\mathrm{E}_1+(1-\phi_1)\phi_2\mathrm{E}_2+\cdots+(1-\phi_1)\times(1-\phi_2)\cdots\phi_M\mathrm{E}_{M+1}) \quad (4)$$

where σ^2 is the variance of driving white noise (WH) and E_i is the matrix representing the covariance for $M+1$ noise models.

Here we use the fractional differencing [11] to construct the covariance matrix of non-Gaussian correlated noise models as in [10], [12] and [18]. The analytical expressions for various stochastic models (e.g., PL, ARFIMA and GGM noise) have been given in [13] and here we only summarize the analytical expressions and their spectral behaviors. Since higher order AR lag polynomial (AR(n), $n > 1$) might actually be associated with signals even though it may give a better fit the overall observational spectrum (for details, see [3]), we only consider ARFIMA(1, d, 0) stochastic model (here we temporally shorten it to ARFI(1) for clarity), which mathematically defined as

$$(1-\phi B)(1-B)^d x_t=w_t \quad (5)$$

where ϕ is the AR lag and d is the fractional integration parameter, which are unknown coefficients need to be estimated; B is the backshift operator defined by $Bx_t = x_{t-1}$; w_i is Gaussian white process with mean zero and variance σ^2. The term $(1-B)^d$ is generalized this expression to fractional differences, which can be interpreted via the binomial series [11]:

$$(1-B)^d=\sum_{i=0}^{\infty}\binom{d}{i}(-1)^i B^i=\sum_{i=0}^{\infty}\frac{\Gamma(i-d)}{\Gamma(i+1)\Gamma(-d)}B^i \quad (6)$$

The covariance function of ARFI(1) with σ normalized unity is given by Hosking [11]:

$$\gamma_k=\frac{1}{1-\phi^2}\frac{\Gamma(1-2d)}{\Gamma(1-d)}\frac{\Gamma(d+k)}{\Gamma(d)\Gamma(1-d+k)}$$

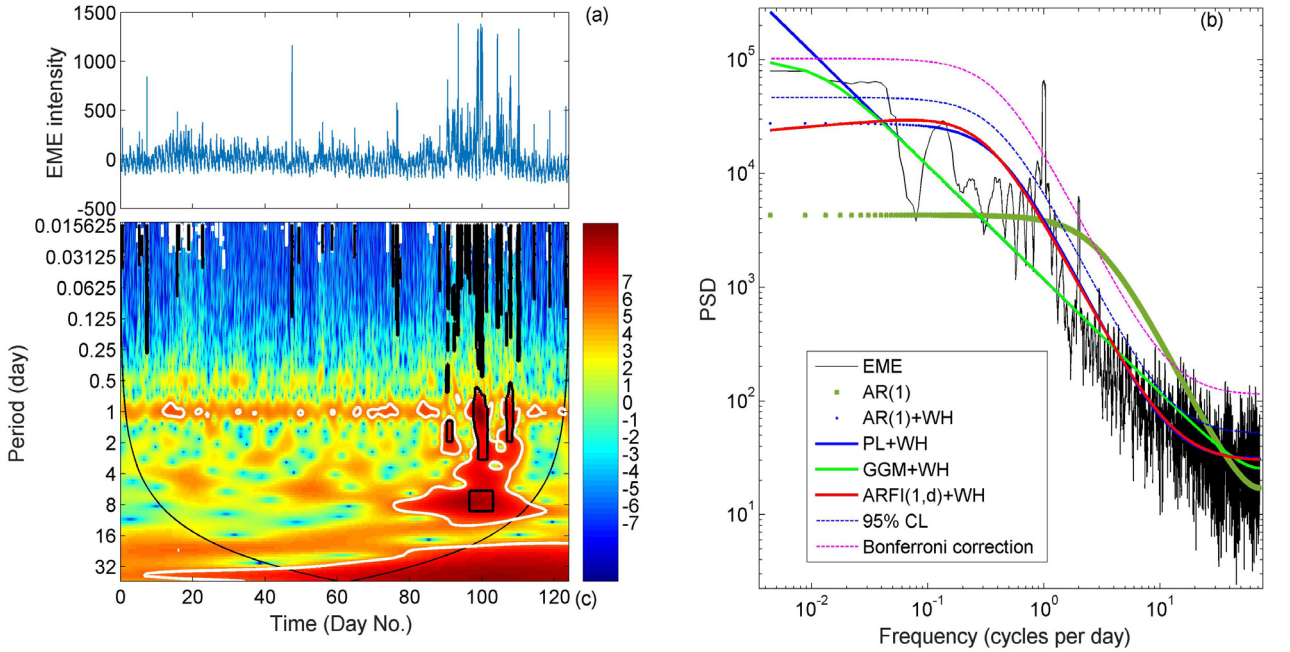

FIGURE 1. Results of spectral analysis on the EME time series. (a) Filtered EME time series in a time resolution of 10 min from Kalimeris *et al.* [20]. (b) MTM spectrum result, where black curve represents the adaptively weighted multitaper spectrum (calculated with the bandwidth parameter is $p = 4$ and taper $K = 7$). Blue and red dashed curves represent the 95% CL and Bonferroni corrected 95% CL based on the preferred noise model with the lowest BIC values. (c) Wavelet spectrum (calculated with a Morlet wavelet with dimensionless frequency $w_0 = 6$). White lines represent the pointwise significant spectral components (95% CL) assuming a traditional AR(1) null, heavy black lines represent the areawise significant spectral components (95% CL with a arealsiglevel of 0.9) assuming the preferred noise background and considering multiple testing effects. The cone of influence (COI), which indicates the region affected by edge effects, is shown with a thick black line. Pointwise significance thresholds are determined from the chi-square test. AR(1) = first-order autoregressive, WH = white noise, PL = power law, GGM = Generalized Gauss Markov, and ARFI(1) = Autoregressive Fractionally Integrated Moving Average (1, d, 0), respectively.

$$\times[F(d+k,1;1-d+k;\phi) + F(d-h,1;1-d-k;\phi)-1] \quad (7)$$

where Γ is the gamma function, $\begin{cases}\Gamma(n+1)=n\Gamma(n)\\ \Gamma(n+1)=n!\end{cases}$; F is the hypergeometric function [19], defined as

$$F(a,b;c;\rho)=\sum_{i=0}^{\infty}\frac{\Gamma(a+i)\Gamma(b+i)\Gamma(c)}{\Gamma(a)\Gamma(b)\Gamma(c+i)i!}\rho^i \quad (8)$$

The one-sided power spectrum density (PSD) for ARFI(1) stochastic model is given by

$$P(f)=\frac{2\sigma^2}{f_s}\frac{[2\sin(\pi f/fs)]^{-2d}}{1+\phi^2-2\phi\cos(2\pi f/f_s)} \quad (9)$$

where f_s is the sample frequency.

For the case of GGM noise, i.e., $(1-\phi B)^d x_t = w_t$, the covariance function with σ normalized unity has the form of

$$\gamma_k=\frac{\Gamma(d+k)\phi^k}{\Gamma(d)\Gamma(1+k)}\times F(d+k,d;1+k;\phi^2) \quad (10)$$

The one-sided PSD for GGM stochastic model is given by

$$P(f)=\frac{2\sigma^2}{f_s[1+\phi^2-2\phi\cos(2\pi f/f_s)]^d} \quad (11)$$

Similarly, we can obtain the covariance function for the pure PL and conventional AR(1) stochastic model with parameters ϕ and d in special cases.

III. APPLICATIONS TO REAL DATA

A. ELECTROMAGNETIC EMISSION (EME) TIME SERIES

We now discuss some real data sets in the prior literature and quantify the performance of our algorithm to examine the evidence for cycles in each. As the first test case we revisit the kHz electromagnetic emission (EME) time series in North–South orientation associated with the Athens' earthquake (M = 5.9, 7 September 1999), which were acquired using a 10 kHz tuned loop antenna installed on a carefully selected mountainous site at Zakynthos Island (37.76° N, 20.76° E), Greece. Here we only focus on the filtered version (starts on 00:00:00 (UT) of May 30, 1999, and finishes on 23:59:59 (UT) of September 29, 1999, covering a period of 123 days with a time resolution of 10 min) of the original EME time series, which has been detailed discussed by Kalimeris *et al.* [20] with ML96 and TC98 method against the hypothesis an AR(1) red noise. In this section, we reanalysis the EME time series (see Fig. 1(a)) with the adaptively weighted multitaper spectrum and TC98 method but using the CLs calculated by our preferred noise background. The relative goodness of fit of the candidate noise models in the data is tested using the minimum Bayesian Information Criterion (BIC) [21]:

$$\text{BIC}=K\cdot\ln[N]+2\ln[L] \quad (12)$$

where K is the sum of parameters estimated, N is the length of observations, and L is the aximum likelihood.

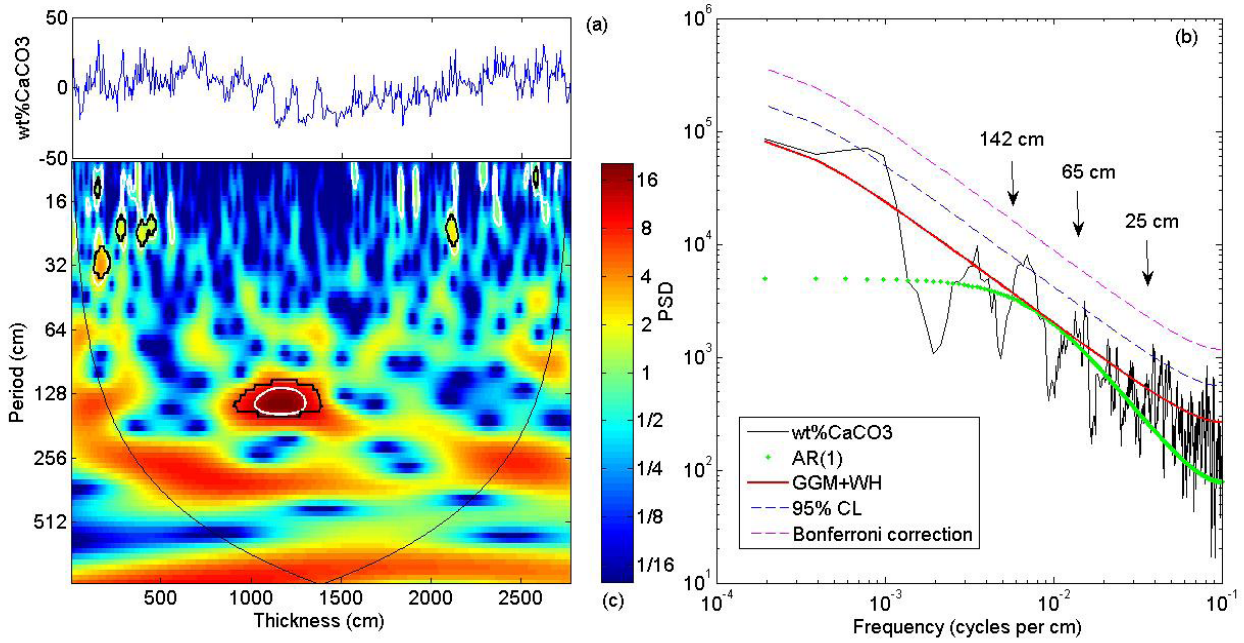

FIGURE 2. Same as Figure 1 but for the wt%CaCO3 data from Suan *et al.* [23]. Bandwidth parameter $p = 2$ and tapers $K = 3$ are used in MTM spectrum. For clarity, only the results of traditional AR(1) and the preferred noise model with the lowest BIC values are provided.

Five alternative noise models in a total of five different combinations (i.e., pure AR(1), AR(1)+WH, PL+WH, GGM+WH, ARFI(1)+WH, respectively) are adopted as possible candidate null hypothesis. Prior to spectral analysis, the original data is linear detrended to improve results at low frequencies, since we note that such a detrending procedure does not alter the MLE estimates that are obtained in time domain. Simply visually compare the spectra of the time series (the bandwidth parameter is $p = 4$ and $K = 7$ tapers were used) and the estimated noise models, we find that the pure AR(1) model is not a good description of the temporal correlation that exists in EME time series, whereas the AR(1)+WH model, which has the lows BIC values, is indeed preferred to characterize this record (see Fig. 1(b)).

We scale the theoretical preferred noise spectrum by using the chi-squared distribution to obtain various CLs (for details, see Appendix A3 in [3]). At these CLs the MTM spectrum indicates spectral features at extra long-scales ($>$ 30 days), diurnal (24h) and semidiurnal (12h) terms are statistically significant, whereas spectral features at long-scales (2-10 days) are not statistical significant at the 95% CL based on a AR(1)+WH null. Our result is partially in agreement with the findings in [20]. Additionally, we find that most spectral features (except those at diurnal and semidiurnal hours) are not statistical significant in the MTM spectrum after applying the Bonferroni correction [22] by dividing the significance level (e.g., $\alpha = 0.05$) by the number of tested data as in [7]. In consistency with the aforementioned MTM methods, Fig. 1(c) shows that extra long-scales variability modes ($>$ 30 days) and oscillatory modes at 3-6 days vanish in the high activity epoch ($98.5 \leq \mathrm{DN} \leq 100.5$) in the areawise significance test ($\alpha = 0.005$), which are based on the area and shape of the significant regions proposed by Maraun *et al.* [15] but modified here by just using the chi-square test (for details, see Equation (18) in TC98) but not the MC simulations to reduce the computation cost. In particular, oscillatory terms between 8 and 10 days become significant at about day number DN = 97, and not at DN = 76 as charmed by Kalimeris *et al.* [20]. We also find that oscillatory terms between 8 and 10 days remain in the high activity scale for approximately 3 days after the main seismic shock occurred at DN = 100.498. Furthermore, we find that the periodicities shorter than 45 min and the intermittent diurnal/semidiurnal oscillatory modes are still stable and significant. Based on these results, it seems plausible that the significant spectral features claimed by Kalimeris *et al.* [20] are artifacts of a poor choice of null "noise" hypothesis and a lack of multiple test correction, and we led to the conclusion that the transition period ($82.6 \leq \mathrm{DN} \leq 90.2$) before the Athens' earthquake (M = 5.9, 7 September 1999) defined by Kalimeris *et al.* [20] may be unreliable. Anyway, our new results with those found in [20] can enhance the preseismic character of the recorded kHz EME time series.

B. WEIGHT-PERCENTAGE CALCIUM CARBONATE (wt%CaCO3) DATA

The second example is the wt%CaCO3 data sampled at 5 cm intervals from an about 30 m Lower Toarcian Peniche section, Portugal, which is drawn from the stratigraphic literature of Suan *et al.* [23]. Using the Blackman-Tukey spectrum

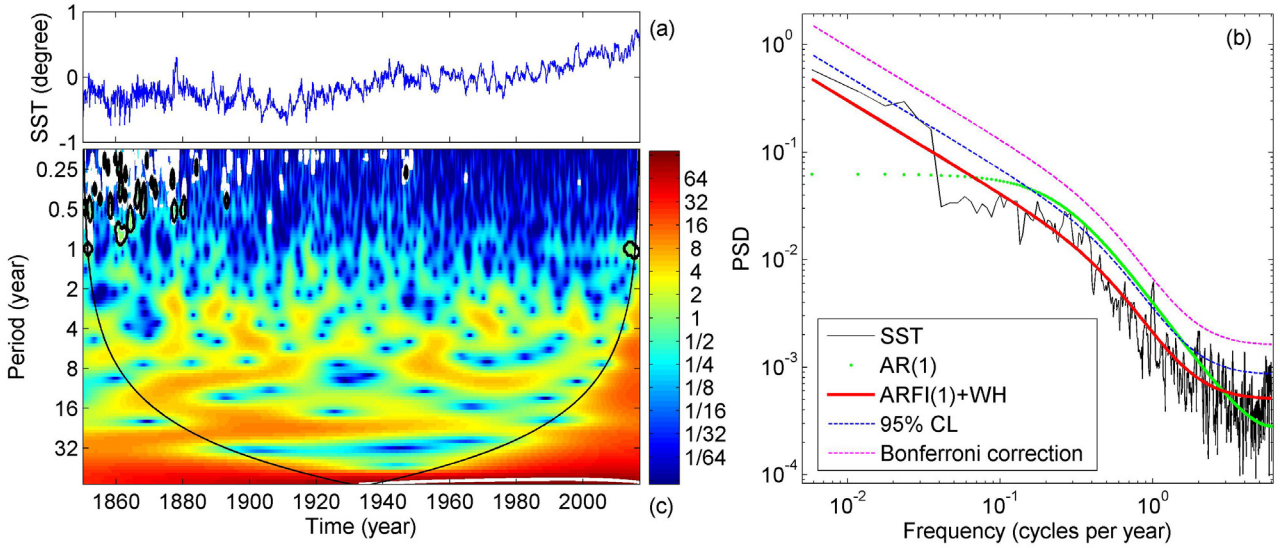

FIGURE 3. Same as Figure 1 but for the monthly sampled global averaged SSTA data from HadSST3. For clarity, only the results of a traditional AR(1) process and the preferred noise model with the lowest BIC values are provided.

with the CLs determined by the ML96 method against the hypothesis an AR(1) process, Suan *et al.* [23] claim to identify several cycles with wavelengths from 23 to 238 cm. However, Vaughan *et al.* [7] reveal that some cycles claimed by Suan *et al.* [23] are artifacts, as evidenced by the calculated 95% CL with the 'Bonferroni correction' and under the assumption than the underlying noise background is a PL. Consequently, we reanalyze the wt%CaCO3 data with our own approach (see Fig. 2(a)). BIC values confirm that in this case an AR(1) process does not provide a reasonable match to the data, whereas the GGM+WH model (actually GGM model since the amplitude of WH is 0), which has the lowest BIC values, is indeed preferred to characterize this record (see Fig. 2(b)). Additionally, we note that our AR(1) model captures the power decay of wt%CaCO3 data worse than that in [23], because the data in [23] are prior linear and 3rd-order polynomial de-trended to reshape the spectral data to match slightly better the assumed AR(1) model. The significance test based on our preferred noise model reveals that three spectral peaks at around 142 cm, 65 cm and 25 cm are exceeding the 95% CL in both MTM. However, these three peaks are not statistical significant in MTM spectrum when taking the Bonferroni correction into account (see Fig. 2(b)). Our MTM result is in agreement with the findings in [7]. However, the cycles with thickness of about 142 cm, 33 cm, and 25 cm are still statistical significant in wavelet spectrum when taking the test multiplicity into account (see Fig. 2(c)). Bear in mind that applying a Bonferroni correction maybe too strict for the stratigraphic data sets with the depth used as a proxy for time (see [24] and [25], for a more detailed discussion of this point). We therefore reiterate that the main cyclicities with cycle thickness of 147 cm and 23 cm claimed in [23] has in fact statistical significance.

C. SEA SURFACE TEMPERATURE

In the past there have been a few publications in which the SST is generally tested against the hypothesis of an AR(1) process. However, Hall and Manabe [26] and Fraedrich *et al.* [27] reveal that the spectra of SST anomaly (SSTA) are generally inconsistent with an AR(1) process. In this case, as the last test case for our method we revisit the Met Office Hadley Centre's SST data set (HadSST3) (available at http://www.metoffice.gov.uk/), which was generated from in situ observations held in the International Comprehensive Ocean Atmosphere Data Set, ICOADS (see http://www.cdc.noaa.gov/coads/). In this section, we only focus on the monthly sampled global average and tropical (20°S-20°N) SSTA (relative to 1961-1990) span from Jan 1850 to Dec 2016. Detailed description of the dataset and its production process can be found in [28] and [29]. Fig. 3(b) confirms that the SST spectra are characterized by a slower but longer increase of the SST variance from inter-annual to decadal time scales, making the global averaged SSTA is significant deviations from the hypothesis a conventional AR(1) process. Dommenget and Latif [30] pointed out that the interaction between the mixed layer and the sub-mixed layer ocean contributes this inconsistent. Moreover, MLE result shows that the global averaged SSTA is characterized by an ARFI(1, 0.4310) +WH process, and the tropical SSTA is characterized by a GGM+WH process with a fractional integration parameter of 1.2882 ± 0.1266. Large fraction of WH is also detected in the MLE covariance matrix (0.65262 for global averaged SSTA and 0.513 for tropical SSTA), revealing that atmospheric disturbances, which is often explained as a WH response in the high frequency band, is a main cause for SST variability. Additionally, both two SSTA spectra have an evident annual peak (see Fig 3(b) and

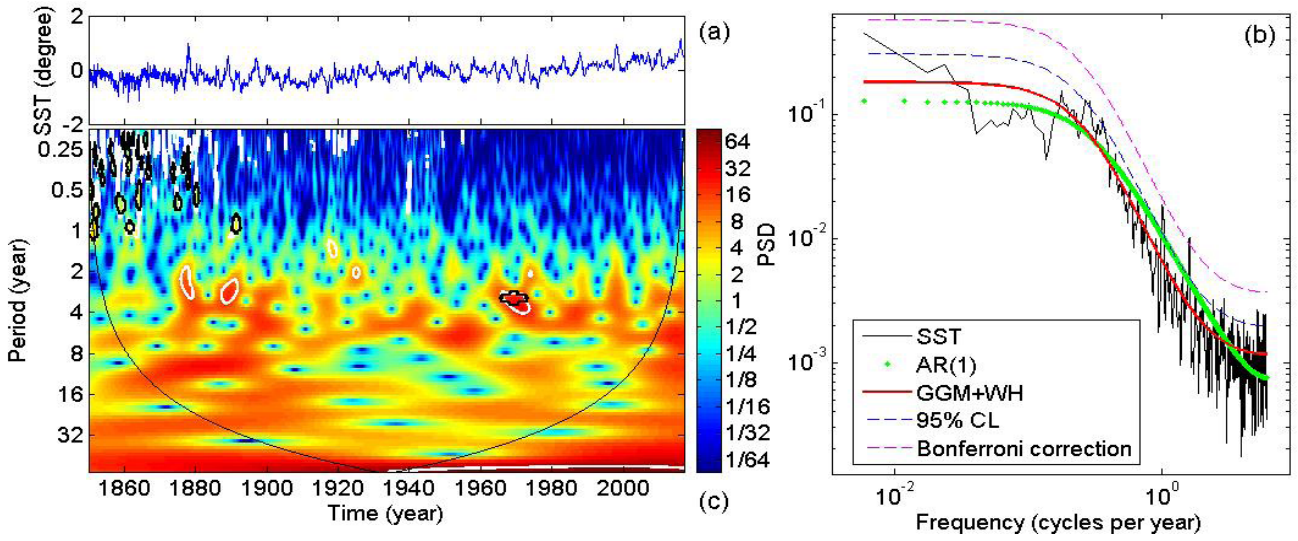

FIGURE 4. Same as Figure 1 and Figure 3 but for the monthly sampled tropical SSTA data from HadSST3.

Fig 4(b)), which is statistical significant at the 95% CL in the MTM spectrum but is not significant when the Bonferroni correction is taken into account. However, it is interested to find that semi-annual peak is a weak or absent in the tropical SSTA spectra, and this peak is instead shifted to slightly lower frequencies located at ∼1.59 cycle per year. This peak is stronger and more statistical significant than that of global average SSTA (see Fig 3(b) and Fig 4(b)), which may be attributed to the local air-sea interaction forcing in the tropics, as revealed by Möller *et al.* [31]. However, interdecadal variability in global average and tropical SSTA cannot be clear distinguished from the wavelet scale at the areawise 95 CL with a multiple testing. Concerning the short time-scales, many significant spectral components are detected in periodicities $\leq$ 1-year even taking the test multiplicity into account, as seen by the successive dark bubbles in the upper left region of the wavelet spectrum in Fig. 3(c) and Fig. 4(c). Moreover, the period between around 1850 and 1880 seems to be distinct from other times, as significance peaks occurs. The physical interpretation of this time-dependent interrelation requires further detailed investigation of possible coupling mechanisms.

IV. CONCLUSION

We have recalled the multitaper and wavelet analyses to significant test for periodic features embedded in noisy data, but extend them with a wider range of noise processes (null hypotheses). An alternative noise estimation method is adopted based on the maximum likelihood estimation (MLE) technique in the time domain, along with the data error covariance constructed using fractional differencing. Bayesian Information Criterion (BIC) is applied to determine which of the candidate noise backgrounds is a preferred fit to the data. The problems due to multiple testing are also investigated. We exemplify this discussion with EME recordings, stratigraphic data, and sea surface temperature anomaly. The importance of checking the noise background is reiterated for accurately estimating the confidence levels of periodic (or quasi-periodic) features. Bear in mind that quantifying the significance of spectral peaks through a strict statistical approach alone is sufficient and additional validating evidences

ACKNOWLEDGMENT

The authors would like to thank Machiel Bos for providing the Hector software for an easy estimation various stochastic models, and to Anastasios Kalimeris and Stelios M. Potirakis for providing the EME recordings. This research is partially benefitted from the Met Office Hadley Centre's data products. The wavelet analysis was performed using some Matlab routines provided by C. Torrence and G. Compo (available at: http://paos.colorado.edu/research/wavelets/) and the SOWAS developed by D. Maraun and J. Laehnemann (available at: http://tocsy.agnld.uni-potsdam.de/wavelets).

REFERENCES

[1] T. Christopher and G. P. Compo, "A practical guide to wavelet analysis," *Bull. Amer. Meteorol. Soc.*, vol. 79, no. 1, pp. 61–78, 1998.
[2] M. Ghil, M. R. Allen, M. D. Dettinger, K. Ide, D. Kondrashov, M. E. Mann, A. W. Robertson, A. Saunders, Y. Tian, F. Varadi, P. Yiou, "Advanced spectral methods for climatic time series," *Rev. Geophys.*, vol. 40, no. 1, pp. 1–3, Feb. 2002.
[3] M. E. Mann and J. M. Lees, "Robust estimation of background noise and signal detection in climatic time series," *Climatic Change*, vol. 33, no. 3, pp. 409–445, Jul. 1996.
[4] M. R. Allen and L. A. Smith, "Monte Carlo SSA: Detecting irregular oscillations in the presence of colored noise," *J. Climate*, vol. 9, no. 12, pp. 3373–3404, Dec. 1996.
[5] S. Vaughan, "A simple test for periodic signals in red noise," *Astron. Astrophys.*, vol. 431, no. 1, pp. 391–403, Feb. 2005.
[6] S. D. P. Williams, Y. Bock, P. Fang, P. Jamason, R. M. Nikolaidis, L. Prawirodirdjo, M. Miller, and D. J. Johnson, "Error analysis of continuous GPS position time series," *J. Geophys. Res. Solid Earth*, vol. 109, no. B3, Mar. 2004, Art. no. B03412.

[7] S. Vaughan, R. J. Bailey, and D. G. Smith, "Detecting cycles in stratigraphic data: Spectral analysis in the presence of red noise," *Paleoceanography*, vol. 26, no. 4, Dec. 2011, Art. no. PA4211.
[8] F. Auchère, C. Froment, K. Bocchialini, E. Buchlin, and J. Solomon, "On the Fourier and wavelet analysis of coronal time series," *Astrophysical J.*, vol. 825, no. 2, p. 110, Jul. 2016.
[9] C. Xu, "Detecting periodic oscillations in astronomy data: Revisiting wavelet analysis with coloured and white noise," *Monthly Notices Roy. Astronomical Soc.*, vol. 466, no. 4, pp. 3827–3833, May 2017.
[10] J. Langbein, "Noise in two-color electronic distance meter measurements revisited," *J. Geophys. Res. B, Solid Earth*, vol. 109, no. 4, Apr. 2004, Art. no. B04406.
[11] J. R. M. Hosking, "Fractional differencing," *Biometrika*, vol. 68, no. 1, pp. 165–176, Apr. 1981.
[12] S. D. P. Williams, "CATS: GPS coordinate time series analysis software," *GPS Solutions*, vol. 12, no. 2, pp. 147–153, Mar. 2008.
[13] M. S. Bos, S. D. P. Williams, I. B. Araújo, and L. Bastos, "The effect of temporal correlated noise on the sea level rate and acceleration uncertainty," *Geophys. J. Int.*, vol. 196, no. 3, pp. 1423–1430, Mar. 2014.
[14] F. Sowell, "Maximum likelihood estimation of stationary univariate fractionally integrated time series models," *J. Econometrics*, vol. 53, nos. 1–3, pp. 165–188, Jul./Sep. 1992.
[15] D. Maraun, J. Kurths, and M. Holschneider, "Nonstationary Gaussian processes in wavelet domain: Synthesis, estimation, and significance testing," *Phys. Rev. E, Stat. Phys. Plasmas Fluids Relat. Interdiscip. Top.*, vol. 75, no. 1, Jan. 2007, Art. no. 016707.
[16] J. Langbein and H. Johnson, "Correlated errors in geodetic time series: Implications for time-dependent deformation," *J. Geophys. Res. B, Solid Earth*, vol. 102, no. B1, pp. 591–603, Jan. 1997.
[17] S. Vaughan and A. C. Fabian, "The high frequency power spectrum of Markarian 766," *Monthly Notices Roy. Astronomical Soc.*, vol. 341, no. 2, pp. 496–500, May 2003.
[18] M. S. Bos, R. M. S. Fernandes, S. D. P. Williams, and L. Bastos, "Fast error analysis of continuous GNSS observations with missing data," *J. Geodesy*, vol. 87, no. 4, pp. 351–360, Apr. 2013.
[19] M. Abramowitz and I. A. Stegun, "Handbook of mathematical functions, with formulas, graphs, and mathematical tables," *J. Appl. Mech.*, vol. 32, p. 239, 1965.
[20] A. Kalimeris, S. M. Potirakis, K. Eftaxias, G. Antonopoulos, J. Kopanas, and C. Nomikos, "Multi-spectral detection of statistically significant components in pre-seismic electromagnetic emissions related with Athens 1999, M = 5.9 earthquake," *J. Appl. Geophys.*, vol. 128, pp. 41–57, May 2016.
[21] G. Schwarz, "Estimating the dimension of a model," *Ann. Statist.*, vol. 6, no. 2, pp. 461–464, 1978.
[22] E. Lehmann, *Testing Statistical Hypothesis*. New York, NY, USA: Springer, 1986.
[23] G. Suan, B. Pittet, I. Bour, E. Mattioli, L. V. Duarte, and S. Mailliot, "Duration of the Early Toarcian carbon isotope excursion deduced from spectral analysis: Consequence for its possible causes," *Earth Planet. Sci. Lett.*, vol. 267, nos. 3–4, pp. 666–679, Mar. 2008.
[24] M. Mudelsee, D. Scholz, R. Röthlisberger, D. Fleitmann, A. Mangini, and E. W. Wolff, "Climate spectrum estimation in the presence of timescale errors," *Nonlinear Processes Geophys.*, vol. 16, no. 1, pp. 43–56, 2009.
[25] S. R. Meyers, "Seeing red in cyclic stratigraphy: Spectral noise estimation for astrochronology," *Paleoceanography*, vol. 27, no. 3, Sep. 2012, Art. no. PA3228.
[26] A. Hall and S. Manabe, "Can local linear stochastic theory explain sea surface temperature and salinity variability?" *Climate Dyn.*, vol. 13, no. 3, pp. 167–180, Mar. 1997.
[27] K. Fraedrich, U. Luksch, and R. Blender, "1/*f* model for long-time memory of the ocean surface temperature," *Phys. Rev. E, Stat. Phys. Plasmas Fluids Relat. Interdiscip. Top.*, vol. 70, no. 3, Sep. 2004, Art. no. 037301.
[28] J. J. Kennedy, N. A. Rayner, R. O. Smith, D. E. Parker, and M. Saunby, "Reassessing biases and other uncertainties in sea surface temperature observations measured *in situ* since 1850: 1. Measurement and sampling uncertainties," *J. Geophys. Res.*, vol. 116, no. D14, pp. 811–840, Jul. 2011.
[29] J. J. Kennedy, N. A. Rayner, R. O. Smith, D. E. Parker, and M. Saunby, "Reassessing biases and other uncertainties in sea surface temperature observations measured *in situ* since 1850: 2. Biases and homogenization," *J. Geophys. Res. Atmos.*, vol. 116, no. D14, pp. 811–840, Jul. 2011.
[30] D. Dommenget and M. Latif, "Analysis of observed and simulated SST spectra in the midlatitudes," *Climate Dyn.*, vol. 19, nos. 3–4, pp. 277–288, Jul. 2002.
[31] J. Möller, D. Dommenget, and V. A. Semenov, "The annual peak in the SST anomaly spectrum," *J. Climate*, vol. 21, pp. 2810–2823, Jun. 2008.

CHANG XU was born in Jiangsu, China, in 1983. He received the B.S. degree in surveying and mapping from the Nanjing University of Technology, Nanjing, China, in 2005, and the M.S. and Ph.D. degrees in geodesy from Hohai University, Nanjing, in 2008 and 2016, respectively.

He is currently an Associate Professor with the Zhejiang University of Water Resources and Electric Power. His current research interests include geodesy, nonparametric statistical methods, and structural health monitoring.

Dr. Xu is a member of IABMAS and IALCCE. He was a recipient of young and middle-aged academic leaders in colleges and universities, Zhejiang, China, in 2017.